

SUPPORTING INFORMATION

Identification of an acyl-enzyme intermediate in a *meta*-cleavage product hydrolase reveals the versatility of the catalytic triad

Antonio C. Ruzzini^{†,‡}, Subhangi Ghosh^{§,‡}, Geoff P. Horsman[‡], Leonard J. Foster[†], Jeffrey T. Bolin^{*,§},
Lindsay D. Eltis^{*,†,||}

[†] Department of Biochemistry and Molecular Biology, University of British Columbia, BC, Canada

[§] Purdue Cancer Research Center and Markey Center for Structural Biology, Department of
Biological Sciences, Purdue University, West Lafayette, IN, USA

^{||} Department of Microbiology and Immunology, University of British Columbia, BC, Canada

Present address

[‡] Department of Chemistry, Wilfrid Laurier University, Waterloo, Ontario, Canada

Author Contributions

[‡] These authors contributed equally to this work.

Corresponding authors

Jeffrey T Bolin – jtb@purdue.edu

Lindsay D Eltis – leltis@mail.ubc.ca

Table of Contents

Experimental Section

Analysis of steady-state kinetic data S2

Results

Table S1. Properties of the crystals, diffraction data, and refinement statistics S2

Table S2. Results of restrained refinements of ES complexes assuming different isomers of HOPDA S3

Figure S1. BphD H265Q:HOPDA²⁻ protomer and secondary HOPDA²⁻ binding site S3

Figure S2. Whole protein LC ESI/MS analysis of BphD WT and H265Q reacted with excess HOPDA S4

Table S3. *b*-series ion fragment matching results from MASCOT search S5

Figure S3. Representative EI/GC/MS analysis of benzoate, HOPDA, and BphD-catalyzed reactions in H₂¹⁸O S6

Table S4. Example of modeling EI/GC/MS data to ¹⁸O incorporation: WT + HOPDA reaction S7

Table S5. Relative abundance of benzoate and HOPDA ion fragments as analyzed by EI GC/MS S8

Figure S4. Representative stopped-flow experiments monitoring turnover of HOPDA by BphD H265Q S9

Table S6. Kinetic binding data of S112A variants mixed in 2:1 molar excess to HOPDA S10

Figure S5. S112A/H265Q:HOPDA²⁻ complex and representative binding kinetics S11

Figure S6. Representative pre-steady state burst of HPD formation during turnover by BphD WT S12

Table S7. Estimated transition state stabilization by the binding energy of MCP hydrolase side chains S12

Figure S7. Comparison of the acetylated-DAC-AT:substrate complex and the benzoylated BphD H265Q S13

EXPERIMENTAL SECTION

Analysis of steady-state kinetic data. Contributions of individual residues to transition state stabilization were estimated from previously measured steady-state kinetic parameters of BphD and MhpC. The analysis was performed as previously described for a C35G variant of tyrosyl-tRNA synthetase¹. Briefly, the specificity constants were compared using the following equation: $\Delta G_R = RT \ln[(k_{cat}/K_m)_{mut} / (k_{cat}/K_m)_{WT}]$, which assumes that the transition state energy is unaffected by substitution, and that the mutated side-chains do not affect productive binding of a second substrate, in this case H₂O.

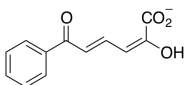
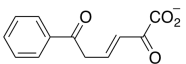
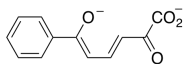
RESULTS

Table S1. Properties of the crystals, diffraction data, and refinement statistics

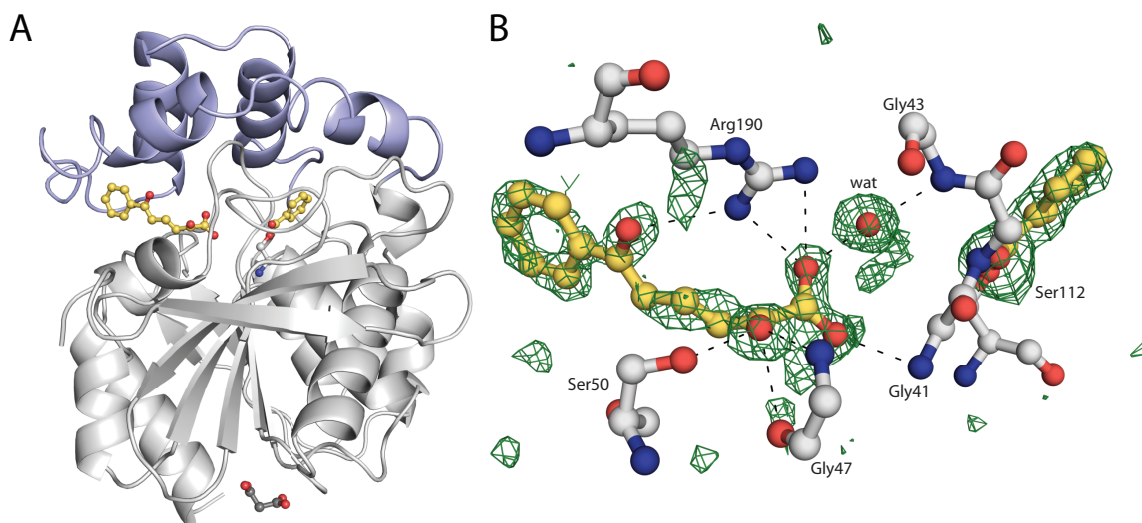
Crystal properties and diffraction data				
Structure	S112A/H265Q	S112A/H265Q:HOPDA	H265Q	H265Q:HOPDA
PDB ID	3V1L	3V1M	3V1K	3V1N
Crystal growth conditions	2.4 M sodium malonate, pH 6.8	2.4 M sodium malonate, pH 7.0	2.4 M sodium malonate, pH 6.6, 3% v/v ethylene glycol	2.4 M sodium malonate, pH 6.4, 10 mM CaCl ₂
Beamline	GM/CA-CAT	LS-CAT	GM/CA-CAT	GM/CA-CAT
	23-ID-B	21-ID-F	23-ID-D	23-ID-D
Wavelength (Å)	1.00	0.98	1.00	1.00
Resolution range ^a (Å)	83.1 - 2.1	82.8 - 1.9	117.8 - 2.1	82.5 - 1.6
Space Group	<i>I</i> 4 ₁ 22	<i>I</i> 4 ₁ 22	<i>P</i> 6 ₄	<i>I</i> 4 ₁ 22
Cell Dimensions (Å)	<i>a</i> = 117.5, <i>c</i> = 87.8	<i>a</i> = 117.1, <i>c</i> = 87.2	<i>a</i> = <i>b</i> = 135.9, <i>c</i> = 65.8	<i>a</i> = 116.6, <i>c</i> = 87.6
Unique reflections	18,100	23,358	39,208	40,883
Multiplicity ^a	7.6 (3.2)	8.1 (5.0)	10.4 (8.2)	14.0 (11.1)
Completeness ^a (%)	97.8 (91)	99.4 (97)	99.9 (100)	99.9 (99.7)
<i>R</i> _{symm} ^a (%)	12.6 (36.7)	7.5 (38.9)	12.2 (94.8)	7.0 (82.4)
Mean ^a <i>I</i> /σ ²	17.5 (2.7)	24.9 (3.8)	21.0 (2.6)	37.9 (2.8)
Refinement				
<i>R</i> _{factor} / <i>R</i> _{free}	0.18 / 0.22	0.18 / 0.22	0.20 / 0.24	0.18 / 0.21
Model content (atoms)				
Non-hydrogen atoms	2401	2382	4623	2446
Protein ^b	2238	2238	4490	2238
Malonate/HOPDA/benzoyl ^c	7 / 0 / 0	7 / 16 (0.6) / 0	7 / 0 / 0	7 / 16 (0.7) / 8
Water oxygens	156	116	126	177
Average <i>B</i> _{factors} (Å ²)				
all atoms	23.9	25.7	42.0	22.0
protein ^b	23.4	25.5	28.6 ^A / 56.0 ^B	21.4
malonate/HOPDA/benzoyl	27.4 / NA / NA	29.4 / 35.0 / NA	42.9 / NA / NA	25.2 / 28.1 / 21.6
waters	30.5	32.0	43.5	30.0
rmsd ^d bond lengths (Å)	0.01	0.01	0.01	0.01
rmsd bond angles (degrees)	1.3	1.2	1.2	1.4

a – Values for highest resolution bin in parentheses, *b* – All chains include residues 4 - 286 except chain A of H265Q, which includes residues 2 - 286. Atoms modeled in two conformations are counted once. *c* – Each ligand was modeled at full occupancy unless otherwise stated in parentheses; one molecule of malonate = 7 atoms, HOPDA = 16 atoms, benzoyl group = 8 atoms. *d* – For the H265Q structure, values for distinct monomers A and B are indicated by superscripts. *e* – rmsd = root-mean-square deviation from restraint targets

Table S2. Results of restrained refinements of ES complexes assuming different isomers of HOPDA^a

Bond Properties		HOPDA isomer ^{b,c}					
		(2 <i>E</i> ,4 <i>E</i>)-2-hydroxy-6-oxo- (2-enol)		(3 <i>E</i>)-2,6-dioxo- (2-keto)		(3 <i>E</i> ,5 <i>Z</i>)-2-oxo-6-oxido-	
							
Variant		S112A/H265Q	H265Q	S112A/H265Q	H265Q	S112A/H265Q	H265Q
C1-C2	Initial	-136	53	-171	52	-171	52
	T-refined	-171	53				
	TP-refined	-149	57	-145	61	-146	63
C2-C3	Initial	-4	-166		-165		-165
	T-refined	64	-165	64		64	
	TP-refined	-2	-166	5	-144	-6	-126
C3-C4	Initial	-170	176	171	175	171	175
	T-refined	171	175				
	TP-refined	-173	149	-180	169	-177	171
C4-C5	Initial	177	-109	134	-110	134	-110
	T-refined	134	-110				
	TP-refined	179	-175	161	-131	175	-152
C5-C6	Initial	168	-175	162	-173	162	-173
	T-refined	162	-173				
	TP-refined	171	-142	178	-179	180	177
C6-CB1	Initial	146	173	149	173	149	173
	T-refined	149	173				
	TP-refined	141	-136	146	176	146	-180

^a – Initial is the value of the angle of the model prior to any refinement. T-refined is the value after tightly restrained torsion angle refinement. TP-refined is the value after refinement restraining both torsion and planarity. All angles are reported in degrees. ^b – Historical tautomer nomenclature is written in parentheses. ^c – The (3*E*,5*Z*)-2-oxo-6-oxido isomer was built into the final model for structures of both ES complexes.



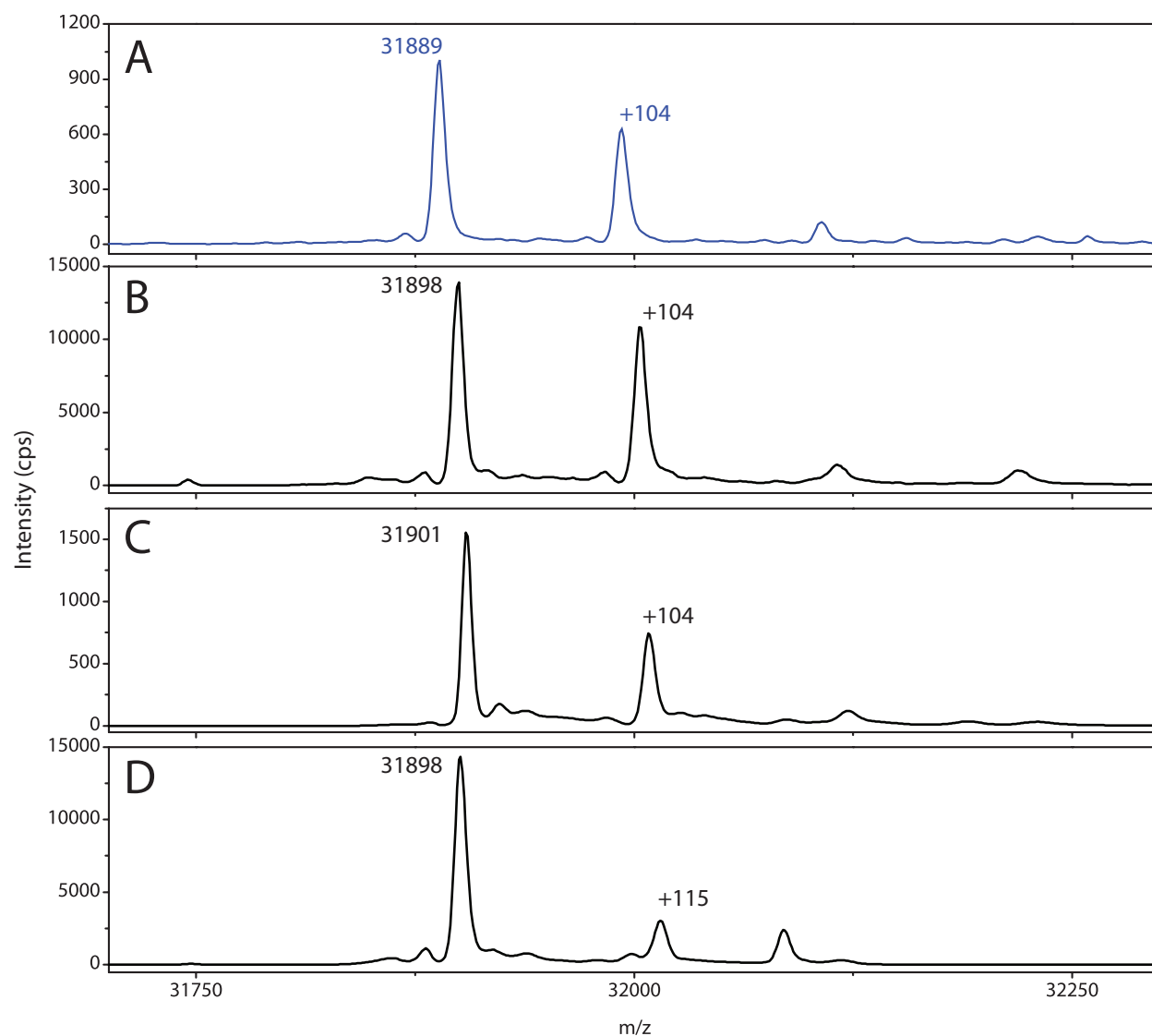


Figure S2. Whole protein LC ESI/MS analysis of H265Q (blue) and WT (black) BphD reacted with HOPDA. Reactions contained 4 μ M enzyme and 20 μ M HOPDA in potassium phosphate ($I = 0.1$ M), pH 7.5 at 25 $^{\circ}$ C. (A) BphD H265Q-catalyzed reaction quenched after 600 ms. The peak areas indicate that ~40% of the enzyme was acylated. (B) WT-catalyzed reaction quenched after 200 ms. Approximately 45% of the enzyme was acylated. (C) WT-catalyzed reaction quenched after 1 s. Approximately 30% of the enzyme was acylated. The apparent mass shift in the spectrum (+3) was due to the higher noise associated with this dataset. (D) WT-catalyzed reaction quenched after 10 s. No peak corresponding to acylated BphD was detected. The +115 peak is consistent with a non-covalent enzyme:HPD adduct, a reaction product that competitively inhibits BphD.

Table S3. *b*-series ion fragment matches to a BphD peptide analyzed by ESI/MS/MS^{a,b,c}

<i>b</i> -series ion	Peptide		
	WT (unmodified)	WT S112-benzoyl	H265Q S112-benzoyl
<i>b</i> ⁹⁺	977.52 / 977.5163	977.54 / 977.5163	977.51 / 977.5163
<i>b</i> ¹⁰⁺	1091.58 / 1091.5592	1091.58 / 1091.5592	1091.57 / 1091.5592
<i>b</i> ¹¹⁺	1178.61 / 1178.5913		1282.64 / 1282.6175
<i>b</i> ¹²⁺	1309.66 / 1309.6317	1413.69 / 1413.6580	1413.73 / 1413.6580
<i>b</i> ¹³⁺	1366.65 / 1366.6532	1470.69 / 1470.6794	
<i>b</i> ¹⁴⁺	1423.67 / 1423.6747	1527.73 / 1527.7009	
<i>b</i> ¹⁵⁺	1494.74 / 1494.7118	1598.74 / 1598.7380	
<i>b</i> ¹⁷⁺	1666.82 / 1666.7966		
<i>b</i> ¹¹⁺⁺	641.83 / 641.8124	589.81 / 589.7993	
<i>b</i> ¹³⁺⁺	735.85 / 735.8434		735.83 / 735.8434
<i>b</i> ¹⁴⁺⁺	764.36 / 764.3541	712.34 / 712.3410	764.33 / 764.3541
<i>b</i> ¹⁵⁺⁺	764.85 / 799.8726		
<i>b</i> ¹⁷⁺⁺	885.97 / 885.9150		
<i>b</i> ¹⁹⁺⁺	999.95 / 999.4785		
<i>b</i> ^{11*++}	581.30 / 581.2860		
<i>b</i> ^{16*++}	789.89 / 789.8701	841.91 / 841.8832	
<i>b</i> ^{17*++}		877.43 / 877.4018	
<i>b</i> ^{11o+}	1160.61 / 1160.5807		
<i>b</i> ^{16o+}	1577.72 / 1577.7489		
<i>b</i> ^{11o++}	580.80 / 580.7940		
<i>b</i> ^{16o++}	789.39 / 789.3781	841.41 / 841.3912	841.37 / 841.3912
<i>b</i> ^{17o++}		876.91 / 876.9098	876.91 / 876.9098
Search Result Statistics			
Ions score	85	63	50
Expect Value	3.8 E-6	0.00057	0.022
Matches (out of 212)	25	34	23
RMS error (ppm)	207	220	276

a – values of the observed fragments based on manual inspection of raw data and fits to Gaussian peaks followed by MASCOT match results

b – MASCOT search of *B. xenovorans* LB400 proteins resulted in a match to the BphD peptide, DIDRAHLVGNSMGGATALNF

c – Symbols * and ° indicate ions with an additional loss of NH₃ and H₂O, respectively.

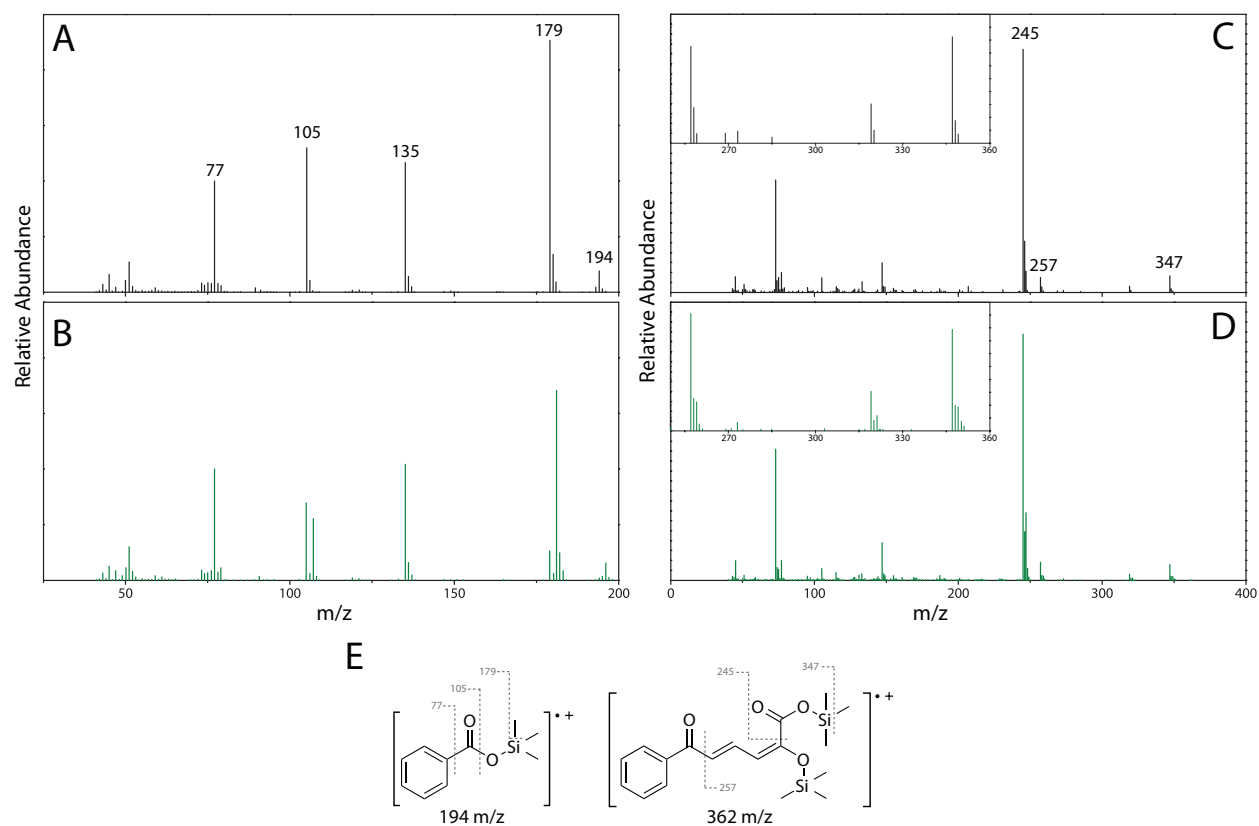


Figure S3. Representative EI/GC/MS analysis of (A) benzoate in H_2O , (B) benzoate derived from BphD-mediated hydrolysis of HOPDA in H_2^{18}O , (C) HOPDA in H_2O , and (D) HOPDA in H_2^{18}O . Inset panels (C and D) highlight the lower intensity HOPDA ion fragments. (E) Illustration of the parent ions and notable fragments.

Table S4. Example of modeling EI/GC/MS data to ¹⁸O incorporation: WT + HOPDA reaction

Observed relative abundance of ions from EI/GC/MS (%)							
m/z	179	180	181	182	183	184	
	[M]	[M+1]	[M+2]	[M+3]	[M+4]	[M+5]	
Control ^a	83.5	12.4	3.9	0.35			
WT + HOPDA ^b	12	2.7	71	10.7	3.6	0.3	
Modeling the relative abundance (R.A.) of benzoate species in the sample (%)							
Model 1: Two species accounting for a single ¹⁸ O incorporation event							
	R.A. [M]	R.A. [M+1]	R.A. [M+2]	R.A. [M+3]	R.A. [M+4]	R.A. [M+5]	Average R.A. ^{c,d}
¹⁶ O/ ¹⁶ O	14	22	16	14			15 ± 1
¹⁶ O/ ¹⁸ O			84	86	92	86	85 ± 1
Model 2: Three species including 3% of doubly ¹⁸ O-incorporated benzoate ^e							
¹⁶ O/ ¹⁶ O	14	22	16	14			15 ± 1
¹⁶ O/ ¹⁸ O			84	86	28	-21	82 ± 3

a – Control values represent the average of all benzoate ion fragments observed in H₂O

b – Benzoate derived from HOPDA incubated with WT BphD for 20 minutes without any pre-incubation

c – The relative abundance of each species (¹⁶O/¹⁸O and ¹⁸O/¹⁸O) was calculated from the observed intensity of each ion (Obs) from the WT reaction and the control (Co) as follows:

$$\text{R.A. } [M]_{16O/16O} = [M]_{\text{Obs}}/[M]_{\text{Co}}$$

$$\text{R.A. } [M+1]_{16O/16O} = [M+1]_{\text{Obs}}/[M+1]_{\text{Co}}$$

$$\text{R.A. } [M+2]_{16O/16O} = ([M]_{\text{Co}} - [M+2]_{\text{Obs}})/([M]_{\text{Co}} - [M+2]_{\text{Co}})$$

$$\text{R.A. } [M+3]_{16O/16O} = ([M+1]_{\text{Co}} - [M+3]_{\text{Obs}})/([M+1]_{\text{Co}} - [M+3]_{\text{Co}})$$

$$\text{R.A. } [M+4]_{16O/16O} = ([M+2]_{\text{Co}} - [M+4]_{\text{Obs}})/([M+2]_{\text{Co}} - [M+4]_{\text{Co}})$$

$$\text{R.A. } [M+5]_{16O/16O} = ([M+3]_{\text{Co}} - [M+5]_{\text{Obs}})/([M+3]_{\text{Co}} - [M+5]_{\text{Co}})$$

$$\text{R.A. of } [M+N]_{16O/18O} = 1 - [M+N]_{16O/16O}$$

d – The averages and errors were weighted based on fragment ion intensity

e – The calculation in Table S4 used a model in which 3% of the benzoate contains two equivalents of ¹⁸O. Ion fragments derived from this species only contribute to the observed signals at M+4 and M+5; no M+6 or M+7 ions were observed.

Table S5. Relative abundance of benzoate and HOPDA ion fragments as analyzed by EI GC/MS

			Relative abundance (%) ^a of benzoate ion fragments (m/z)					¹⁸ O incorporation ^b	
Sample and Incubation time			105 [M]	106 [M+1]	107 [M+2]	108 [M+3]	109 [M+4]		
benzoate	300 min	H ₂ O	92 ± 1	7 ± 1	1.0 ± 0.1				
		H ₂ ¹⁸ O	92.2 ± 0.2	6.7 ± 0.1	1.1 ± 0.1			ND	
WT +	300 min	H ₂ O	92.3 ± 0.1	6.6 ± 0.2	1.1 ± 0.1				
benzoate		H ₂ ¹⁸ O	91.5 ± 0.7	7.2 ± 0.5	1.3 ± 0.2			ND	
WT +	20 min	H ₂ O	92.2 ± 0.4	6.8 ± 0.8	1.0 ± 0.4				
HOPDA		H ₂ ¹⁸ O	53 ± 2	4.9 ± 0.4	39 ± 3	2.7 ± 0.2	0.3 ± 0.2	42 ± 1%	
WT +	5 min PI	H ₂ O	92 ± 2	7 ± 1	1.0 ± 0.3				
HOPDA	20 min rxn	H ₂ ¹⁸ O	52.9 ± 0.3	5.5 ± 0.9	38 ± 1	3.1 ± 0.2	0.17 ± 0.02	42 ± 2%	
WT +	20 min PI	H ₂ O	91 ± 2	8 ± 1	0.9 ± 0.4				
HOPDA	20 min rxn	H ₂ ¹⁸ O	52.5 ± 0.6	4.8 ± 0.3	38.5 ± 0.4	3.8 ± 0.1	0.29 ± 0.03	43 ± 2%	
			179 [M]	180 [M+1]	181 [M+2]	182 [M+3]	183 [M+4]	184 [M+5]	
benzoate	300 min	H ₂ O	83.2 ± 0.6	12.9 ± 0.5	3.4 ± 0.1	0.44 ± 0.08			
		H ₂ ¹⁸ O	83.1 ± 0.5	12.4 ± 0.3	4.1 ± 0.1	0.4 ± 0.2			ND
WT +	300 min	H ₂ O	84.1 ± 0.4	11.9 ± 0.4	3.6 ± 0.1	0.31 ± 0.01			
benzoate		H ₂ ¹⁸ O	83 ± 0.2	12.3 ± 0.1	4.3 ± 0.1	0.4 ± 0.04			ND
WT +	20 min	H ₂ O	84 ± 1	12 ± 1	3.9 ± 0.1	0.3 ± 0.1			
HOPDA		H ₂ ¹⁸ O	12 ± 1	2.7 ± 0.1	71 ± 2	10.7 ± 0.5	3.6 ± 0.1	0.3 ± 0.1	85 ± 1%
WT +	5 min PI	H ₂ O	82.7 ± 0.9	12 ± 1	4.4 ± 0.5	0.4 ± 0.1	0.23 ± 0.01		
HOPDA	20 min rxn	H ₂ ¹⁸ O	14 ± 3	3.9 ± 0.3	68 ± 2	11 ± 1	3.1 ± 0.1	0.3 ± 0.2	80 ± 2%
WT +	20 min PI	H ₂ O	82.7 ± 0.1	12.8 ± 0.4	4.0 ± 0.4	0.33 ± 0.07	0.12 ± 0.04		
HOPDA	20 min rxn	H ₂ ¹⁸ O	16.7 ± 0.4	3.3 ± 0.2	65 ± 1	10.0 ± 0.1	4 ± 1	0.5 ± 0.2	79 ± 2%
			193 [M-1]	194 [M]	195 [M+1]	196 [M+2]	197 [M+3]	198 [M+4]	
benzoate	300 min	H ₂ O	15.7 ± 0.1	70.2 ± 0.7	11.2 ± 0.3	3 ± 1			
		H ₂ ¹⁸ O	18 ± 2	65.6 ± 0.4	12.6 ± 0.1	3 ± 1			ND
WT +	300 min	H ₂ O	15.5 ± 0.3	69 ± 1	12 ± 2	4.0 ± 0.7			
benzoate		H ₂ ¹⁸ O	14.3 ± 0.8	69.5 ± 0.3	11.8 ± 0.3	3.9 ± 0.4	0.39 ± 0.06		ND
WT +	20 min	H ₂ O	17 ± 5	66 ± 1	11 ± 2	5 ± 1			
HOPDA		H ₂ ¹⁸ O	3 ± 1	11 ± 4	15 ± 2	57 ± 8	11 ± 2	2.7 ± 0.8	85 ± 4 %
WT +	5 min PI	H ₂ O	16 ± 2	69 ± 2	11 ± 4	3 ± 5			
HOPDA	20 min rxn	H ₂ ¹⁸ O	3.0 ± 0.4	15 ± 1	12 ± 2	55 ± 1	11.5 ± 0.8	3.0 ± 0.9	72 ± 9 %
WT +	20 min PI	H ₂ O	14 ± 3	71 ± 1	10.7 ± 0.1	5 ± 1			
HOPDA	20 min rxn	H ₂ ¹⁸ O	4 ± 1	10 ± 1	12.5 ± 0.4	59 ± 2	10 ± 1	4.4 ± 0.1	80 ± 10 %
			245 [M]	246 [M+1]	247 [M+2]	248 [M+3]	249 [M+4]	250 [M+5]	
HOPDA	20 min	H ₂ O	78 ± 2	16.0 ± 0.2	5 ± 2	0.5 ± 0.2			
		H ₂ ¹⁸ O	65.0 ± 0.1	12.7 ± 0.2	17.9 ± 0.1	3.2 ± 0.1	1.0 ± 0.2	0.12 ± 0.01	18 ± 1%
			257 [M]	258 [M+1]	259 [M+2]	260 [M+3]	261 [M+4]		
HOPDA	20 min	H ₂ O	71 ± 5	22 ± 5	6.7 ± 0.1				
		H ₂ ¹⁸ O	62.3 ± 0.3	15 ± 3	18 ± 8	3.1 ± 0.1	1.1 ± 0.1		17 ± 1 %
			347 [M]	348 [M+1]	349 [M+2]	350 [M+3]	351 [M+4]		
HOPDA	20 min	H ₂ O	73 ± 6	18 ± 2	8 ± 2	1 ± 1			
		H ₂ ¹⁸ O	58 ± 3	17 ± 2	16 ± 2	6.3 ± 0.8	2 ± 1		17 ± 5%

^a – errors for relative abundance measurements are a standard deviation from two replicates

^b – errors for ¹⁸O incorporation represent the root mean square error from fitting the experimentally observed data to a single ¹⁸O incorporation or to a model that accounts for 2% incorporation of a second ¹⁸O equivalent in parentheses

^c – overall rms error based on weighted residual plot analysis, where residual = predicted % intensity from model – observed value

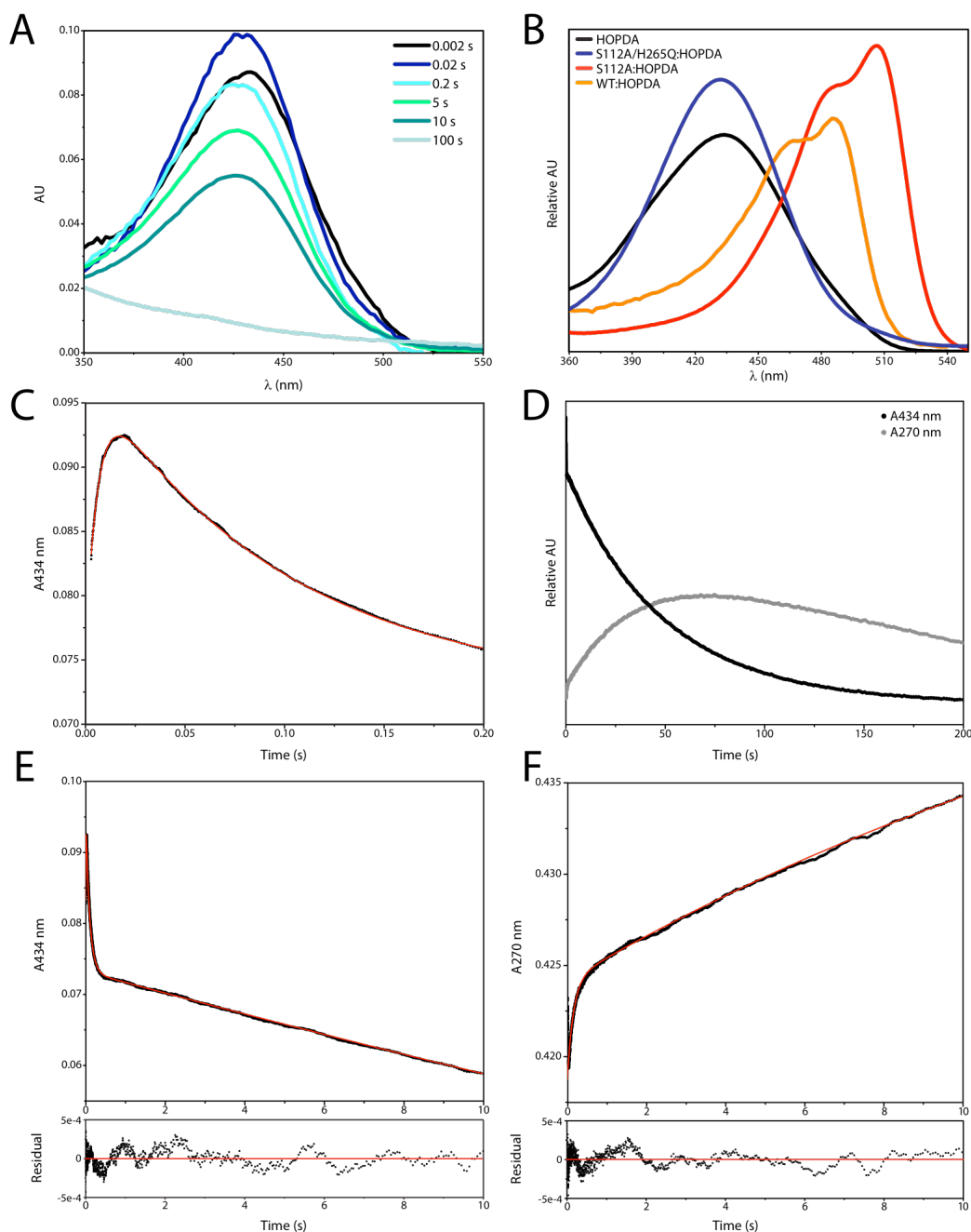


Figure S4. Representative stopped-flow experiments performed in potassium phosphate ($I = 0.1$ M), pH 7.5 at 25 °C. (A) Turnover of 4 μ M HOPDA by 8 μ M BphD H265Q monitored using a photodiode array (note that HOPDAs photodecay under these conditions causing the apparent acceleration of rate constants). (B) The visible absorption spectra of ES complexes in solution. (C) Expanded view of the first 0.2 s during turnover of 4 μ M HOPDA by 8 μ M BphD H265Q. (D) Turnover of 4 μ M HOPDA by 8 μ M BphD H265Q monitored for 200 s, the normalized relative ΔA_{434} nm and ΔA_{270} nm are shown in black and grey, respectively, in order to demonstrate the reactions goes to completion under these conditions. (E) Turnover of 4 μ M HOPDA by 8 μ M BphD H265Q monitored at 434 nm for 10 s. Traces were fit from 0.003 to 10 s with a triple exponential equation (fit in red). The residual is shown below. (F) Turnover of 4 μ M HOPDA by 8 μ M BphD H265Q monitored at 270 nm for 10 s. Traces were fit from 0.02 to 10 s with a triple exponential equation (fit in red). The residual is shown below.

Table S6. Kinetic binding data of S112A variants mixed in 2:1 molar excess to HOPDA^a

Enzyme	λ (nm)	Formation of ES ^{red} or ES ^{planar}						λ_{max} (nm)	$t_{1/2}$ (h)
		k_1 (s ⁻¹)		k_2 (s ⁻¹)		k_3 (s ⁻¹)			
		[% Amp]		[% Amp]		[% Amp]			
S112A ^b	492	~ 500	[85]	76	[11]	0.92	[4]	488 / 506	4.4
S112A/H265A ^b	434	220	[69]	22	[22]	0.34	[9]	432	ND
S112A/H265Q	434	114 ± 8	[39]	32 ± 2	[38]	0.78 ± 0.02	[22]	432	31

^a – all rates are associated with increasing absorptivity at the stated wavelength.^b – data was taken from Horsman *et al* (2007)².

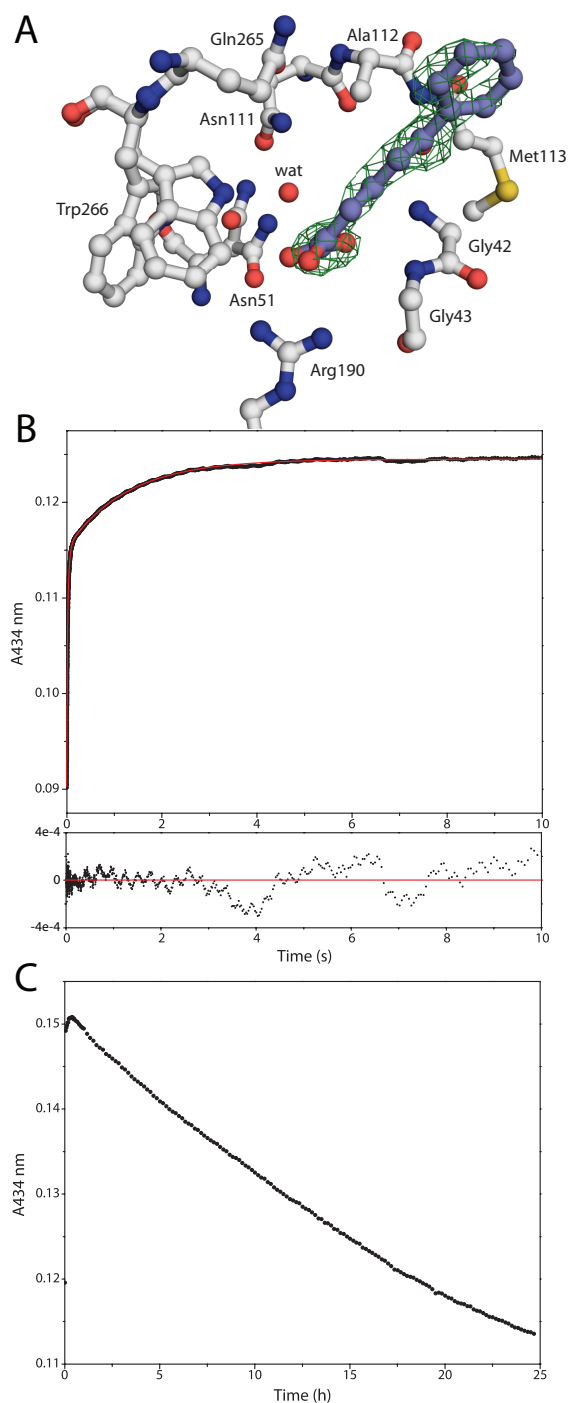


Figure S5. (A) Ball-and-stick representation of the BphD S112A/H265Q:HOPDA²⁻ complex active site, including the unbiased Fo-Fc map (green) for the substrate, contoured at 3σ. Polar contacts are shown using dashed lines. Hydrophobic interactions between the ligand and Ala112, Gly138, Ile153, Leu156, Phe175, Leu213, Trp216, Val240, and Trp 266 have been omitted for simplicity. (B) Representative stopped-flow replicate showing the binding of HOPDA²⁻ to S112A/H265Q in potassium phosphate (I = 0.1 M), pH 7.5 at 25 °C. (C) Representative trace used for estimating the half-life of the S112A/H265Q:HOPDA²⁻ complex.

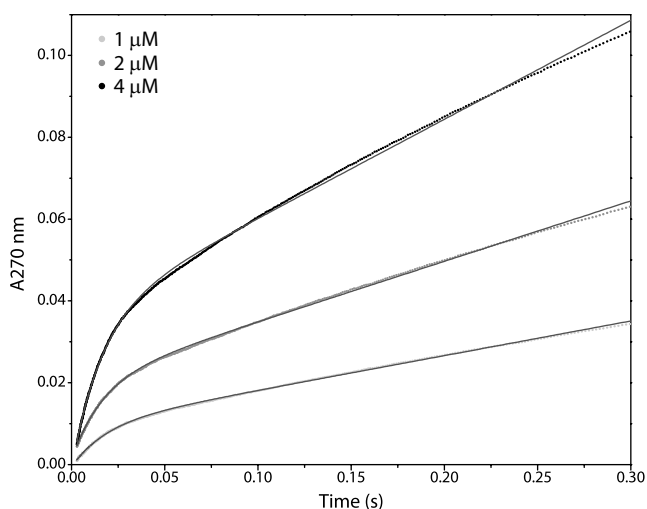


Figure S6. Representative stopped-flow experiments demonstrating a pre-steady state burst of HPD formation by BphD WT in potassium phosphate buffer ($I = 0.1$ M), pH 7.5 at 25 °C. The slight divergence from linearity in the traces can be explained by substrate depletion, which was $\sim 18\%$ after 0.5 s at 4 μM enzyme. Consequently, product accumulation and inhibition ($K_{\text{ic HPD}} \sim 80$ μM , $K_{\text{iu HPD}} \sim 120$ μM , $K_{\text{ic benzoate}} \sim 160$ μM), and non-enzymatic enolization of HPD, associated with a decay of the signal at 270 nm ($k \sim 0.6$ s^{-1}), likely accounts for the reduction in the apparent steady-state rate with increasing enzyme concentration³.

Table S7. Estimated transition state stabilization by the binding energy of MCP hydrolase side chains to HOPDA.

Enzyme	$k_{\text{cat}}/K_{\text{m}}$ ($\text{M}^{-1}\text{s}^{-1}$)	$ \Delta G_{\text{R}} $ (kcal mol^{-1})	Ref
BphD wild type, pH 7.5	3.2×10^6		4
S112C	9.5×10^4	2.1	3
BphD wild-type, pH 8.0	3.3×10^6		5
R190Q	5.7×10^2	5.1	5
R190K	2.8×10^3	4.2	5
MhpC, pH 8.0	4.1×10^6		5
N109A	3.3×10^4	2.9	5
N109H	1.9×10^4	3.2	5
F173G	1.3×10^4	2.0	5
F173D	2.6×10^4	3.0	5
R188Q	1.4×10^3	4.7	5
R188K	1.9×10^4	3.2	5
C261A	2.9×10^6	0.2	5
W264G	2.1×10^4	3.1	5

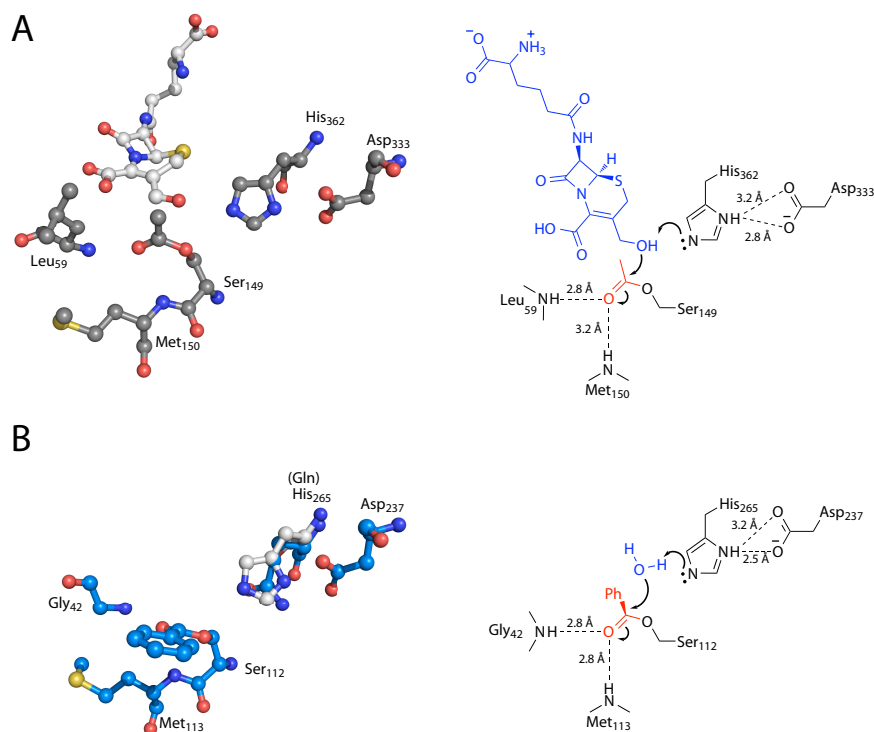


Figure S7. (A) *Left*. Ball-and-stick representation of the acetylated DAC-AT:deacetylcephalosporin C active site (PDB ID: 2VAV Chain L⁶). *Right*. Interpretation of the chemical reaction leading to acetylation by DAC-AT. (B) *Left*. Ball-and-stick representation of the benzoylated BphD H265Q active site, and superposition of His265 from 2OG1 chain B. *Right*. By analogy, the activation of water by the His-Asp dyad is drawn in context of the MCP-hydrolase mechanism.

REFERENCES

1. Wilkinson, A. J.; Fersht, A. R.; Blow, D. M.; Winter, G., *Biochemistry* **1983**, 22 (15), 3581-6.
2. Horsman, G. P.; Bhowmik, S.; Seah, S. Y.; Kumar, P.; Bolin, J. T.; Eltis, L. D., *J Biol Chem* **2007**, 282 (27), 19894-904.
3. Horsman, G. P.; Ke, J.; Dai, S.; Seah, S. Y.; Bolin, J. T.; Eltis, L. D., *Biochemistry* **2006**, 45 (37), 11071-86.
4. Bhowmik, S.; Horsman, G. P.; Bolin, J. T.; Eltis, L. D., *J Biol Chem* **2007**, 282 (50), 36377-85.
5. Li, C.; Li, J. J.; Montgomery, M. G.; Wood, S. P.; Bugg, T. D., *Biochemistry* **2006**, 45 (41), 12470-9.
6. Lejon, S.; Ellis, J.; Valegard, K., *J Mol Biol* **2008**, 377 (3), 935-44.